

S.J. Lambert · J. Sheng · J. Boyle

Winter cyclone frequencies in thirteen models participating in the Atmospheric Model Intercomparison Project (AMIP1)

Received: 11 August 2000 / Accepted: 25 September 2001 / Published online: 22 December 2001
© Springer-Verlag 2001

Abstract Various aspects of the simulated behaviour of cyclones in thirteen models participating in the AMIP1 exercise are presented. In the simulation of the winter climatological mean sea level pressure field for the Northern Hemisphere, the models produce reasonable simulations of the “semi-permanent” features of the climatology. The greatest departures from the observed climatology occur near the exit regions of the oceanic storm tracks; i.e., over northwestern North America, over and to the west of the British Isles and in the Mediterranean. The departures in the three geographical areas are very systematic in that at least eleven of the models exhibit similar departures from observations. In the Southern Hemisphere the intensity of the circumpolar trough is generally well simulated but positioned slightly too far north. Most models exhibit errors south of Africa, New Zealand, and South America. The simulations of the cyclone events show that the models are reasonably successful in reproducing the large-scale aspects of observed cyclone events but deficiencies in the details of the simulations are apparent. The paucity of simulated events to the south of the Alps and to the east of the

Rockies suggests that the models have difficulty simulating lee cyclogenesis. Over much of North America, the models have difficulty simulating the correct level of synoptic activity as demonstrated by the low numbers of both cyclone events and anticyclone events. The models have difficulty simulating the distribution of cyclone events as a function of central pressure. The most common problem is that the models exhibit an ever increasing deficit of events with decreasing central pressure. This problem is more apparent in the Southern Hemisphere than in the Northern Hemisphere and does not appear to be resolution dependent. There is an apparent ENSO signal in the observed Northern Hemisphere interannual variability of intense winter cyclone events. With the exception of ECMWF, the models fail to reproduce this phenomenon. There is some evidence that the models do indeed respond to the interannual variability in the SSTs, but the response tends to be negatively correlated with that of the real atmosphere. In the Southern Hemisphere, there does not appear to be ENSO-induced interannual variability in the observed numbers of cyclone events. Consequently, it could be argued that the models have been reasonably successful in the Southern Hemisphere since they, like the observations, do not exhibit any ENSO-induced interannual variability.

The authors have written this article on behalf of the following participating AMIP1 Modelling Groups: Bureau of Meteorology Research Centre; Canadian Centre for Climate Modelling and Analysis; Center for Ocean-Land-Atmosphere Studies; Commonwealth Scientific and Industrial Research Organisation; Colorado State University; Dynamical Extended Range Forecasting; European Centre for Medium-Range Weather Forecasts; Goddard Laboratory for Atmospheres; Goddard Space Flight Center; Meteorological Research Institute; Recherche en Prévision Numérique; UK Universities' Global Atmospheric Modelling Programme; United Kingdom Meteorological Office.

S.J. Lambert (✉) · J. Sheng
Canadian Centre for Climate Modelling and Analysis,
Meteorological Service of Canada, Victoria, Canada
E-mail: Steve.Lambert@ec.gc.ca

J. Boyle
Program for Climate Model Diagnosis and
Intercomparison Lawrence Livermore National
Laboratory Livermore, USA

1 Introduction

The goal of intercomparison studies, of which only one is the Atmospheric Model Intercomparison Project (AMIP), is the improvement of model simulations. Typically, these intercomparisons are pursued by performing various diagnostic calculations on the outputs from a group of models in order to document similarities and differences among models and, if reliable data are available, to compare their simulations to observations. In the AMIP1 exercise, ten-year simulations were performed using observed sea surface temperatures (SSTs) and sea-ice extent for the period January 1, 1979 to

December 31, 1988. A complete discussion of the AMIP1 experimental design is given in Gates (1992).

The behaviour of cyclones in general circulation models (GCMs) is an important feature of real and simulated atmospheres. Cyclones are usually accompanied by cloudiness and precipitation and are often associated with extreme weather events. They are responsible for much of the poleward heat transport and if projections of future climates made by GCMs are to be credible, it is important that cyclone behaviour be simulated with a high degree of fidelity.

In the present study, model simulations of the winter cyclone event climatologies for the Northern and the Southern Hemisphere extra-tropics are examined. The summer season is not considered because of its much lower level of synoptic activity. When models are under development, the monthly or seasonally averaged mean sea level pressure (MSLP) field is always examined; however, the day-to-day behaviour is rarely considered. Consequently, the model parametrizations have not been adjusted to improve the simulation of cyclone behaviour. In this respect, it can be argued that diagnostic calculations based on fields which were not examined during the development of the models might be a more stringent test of model performance. In addition, the number of cyclone events is sensitive to the SSTs. Lambert (1996) showed that there is a noticeable ENSO signal in the observed intense winter cyclone event frequencies. This makes the cyclone event climatology particularly relevant in diagnosing and evaluating the AMIP1 models which are forced by observed interannually varying SSTs and sea-ice extent.

2 Observation-based data

The primary observation-based data used for the intercomparison are the European Centre for Medium-Range Weather Forecasts Reanalyses (ECMWF/ERA). The production of these data is described in Gibson et al. (1997). Additional data for the Northern Hemisphere are the NMC Operational Analyses (Trenberth and Olson 1988) and the NCEP/NCAR reanalyses (Kalnay et al. 1996). A processing error makes the latter analyses unsuitable for use near the surface in the Southern Hemisphere. Between 1979 and 1993, NCEP assimilated the synthetic PAOBS observations with incorrect longitudes as discussed in Kistler et al. (2001). The quality control procedure removed about half of the incorrectly positioned reports but the remainder were used in the analyses. (The PAOBS data were not used in the ECMWF/ERA analyses.)

Since one of the models in this study is an ECMWF model, it might be perceived that the ECMWF model could benefit, especially in the Southern Hemisphere where the data density is relatively low, because a later version is used in the reanalysis data assimilation system. Kistler et al. (2001) reported on the results of forecast experiments for both the Northern and the Southern Hemispheres using the NCEP Reanalysis data as initial conditions. Their results showed that without the inclusion of the satellite data in the analyses, the forecast skill in the Southern Hemisphere was noticeably lower than that of the Northern Hemisphere. If the satellite data were used, then the skill in both hemispheres was comparable. One can conclude that if satellite data are available then there are sufficient data to define the state of the atmosphere and that the influence of the ‘first-guess’ field used in the assimilation

cycle is minimal. The satellite data were available from 1979 onward and they were also used in the ERA analyses. This indicates that the use of the ERA analyses for verification does not present any advantage to the ECMWF model.

The observation-based datasets were available on latitude-longitude grids and were first interpolated to 96 by 48 point Gaussian grids, then transformed to spectral coefficients with a triangular truncation at 32 waves and finally synthesized onto polar stereographic grids with a spacing of 381 km at 60 degrees latitude.

3 Participating models

The models participating in the AMIP1 exercise employ various physical parametrization schemes and computational procedures. The models use different horizontal and vertical representations with a wide range of resolutions. The models are described in detail in Phillips (1994). High frequency MSLP data were available from the 13 models which are listed in Table 1. This table gives the models’ horizontal and vertical representations and resolutions as well as the grids on which their data were received. Data were available every 12 h except for the COLA and DERF models for which data were available every 24 h.

Two pairs of models are linked because they have a common ancestor. The GLA and GSFC models evolved from the same model as is the case for the ECMWF and the UGAMP models. For the GLA-GSFC pair, the subsequent evolution from the common model has resulted in many differences, such as the vertical resolution and layering, initialization data, the dynamics and radiation time steps, time filtering, cloud emissivity, convection scheme, cloud formation, snow and ice treatment, surface albedo, and land surface processes. These differences complicate the attribution of model performance to model formulation. In the case of ECMWF-UGAMP there has been little change from the parent model. The difference between the two models is in the treatment of convection. The ECMWF model uses a Tiedtke scheme (Tiedtke 1989) while the UGAMP model uses the Betts-Miller scheme (Betts and Miller 1994). Even with this high degree of similarity, caution must be exercised in attributing differences in the results between these two models to their convective formulations.

The model data were transformed to a common grid in order to facilitate intercomparison. The spectral models whose data were received on Gaussian grids were transformed to spectral coefficients with the same resolution as the model which produced the data. The spectral fields were then synthesized onto Northern and Southern Hemisphere polar stereographic grids with a grid spacing of 381 km at 60 degrees latitude. The grid point models whose data were received on latitude-longitude grids were first interpolated to 96 by 48 point Gaussian grids, then spectrally analyzed to spectral coefficients with a triangular truncation at 32 waves and finally synthesized onto the polar stereographic grids.

4 Analysis

There are two types of cyclone frequency climatologies; cyclone track climatologies and cyclone event climatologies. Historically, these have been extracted manually by examining a long series MSLP analyses. The cyclone track climatology is extracted by mapping all the cyclone trajectories in a geographical region over a period of time. The area under consideration is divided into analysis “boxes” (typically grid squares) and the number of cyclone trajectories that pass through each grid square are counted (e.g. Whittaker and Horn 1984). Such analyses are helpful in identifying regions of high cyclone activity, preferred directions taken by lows and identifying long-term trends and variability. In this method, each cyclone is counted only once in each grid square along its track. A rapidly moving cyclone will be counted in exactly the same manner as a slowly moving cyclone and as a consequence

this method does not give an indication of the duration of weather associated with mid-latitude low pressure systems. There is also a subtle bias in this procedure as pointed out by Taylor (1986) who showed that the cyclone track frequency depends on the orientation of the cyclone tracks and the grid squares.

The second method of analysis counts the number of cyclones in each analysis box over a given period of time. As a result, slowly moving lows can be counted more than once in an analysis box and rapidly moving cyclones will not necessarily be counted in all the analysis boxes along its path (Petterssen 1956). This method also will identify regions of increased cyclone activity, provide information on the preferred trajectories, and can show long-term trends. In addition, as a result of the multiple counting, it does provide an indication of the frequency of weather, such as cloudiness and precipitation, that are typically associated with cyclones.

In order to extract cyclone climatologies from many model simulations it is a practical necessity that an objective computer-based procedure be used, since manual procedures are too time consuming to use in the intercomparison of models. A variety of procedures have been developed for the automatic identification of midlatitude cyclones. The simplest of these is described in Lambert (1988) in which the sole criterion for the identification of a cyclone is a minimum in the 1000 mb geopotential or MSLP field. The advantage of this method is that it is economical to use and conceptually straightforward and identifies regions of high cyclone activity. A disadvantage is that the procedure will identify features which cannot be considered mid-latitude cyclones such as thermal

lows and minima in the pressure or height fields resulting from extrapolation under high terrain. In an attempt to address the problem of inclusion of these spurious lows when using only the minimum in the pressure field, procedures have been developed which use additional criteria for the identification of cyclones. König et al. (1993) and Trigo et al. (1999) employed an additional requirement that the Laplacian of the pressure field at the cyclone's centre must exceed a threshold value. Although this procedure is effective in reducing spurious events, there will be a few true events which will not satisfy the criteria and will not be enumerated. This leads to a subjective determination of the threshold in an attempt to maximize the removal of spurious events and minimize the removal of true events. A further disadvantage is that the threshold value depends on the type and resolution of the grid used to extract the cyclone event counts. Somewhat different identification criteria were used by Sinclair and Watterson (1999) to identify cyclones. They computed the vorticity from the smoothed 1000 mb height field and a cyclone event was defined as the occurrence of a vorticity maximum above a certain threshold. In addition to being sensitive to the threshold value, it is also sensitive to the smoothing procedure and the method can produce spurious counts in regions of strong horizontal shear.

The difficulties posed by the counting procedures outlined have lead to a another widely used procedure. This involves selecting an easily diagnosed field from the model simulation, for which reliable observational estimates are available, as a proxy for cyclone activity; (see e.g. Blackmon 1976; Lau 1988; Wallace et al. 1988).

Table 1 Participating AMIP Models

Modelling group	Resolution				Data grid
	Horizontal		Vertical		
Bureau of Meteorology Research Centre, Australia (BMRC)	Spectral	R31	Sigma	9	GG 96 × 78
Canadian Climate Centre, Canada (CCC)	Spectral	T32	Hybrid	10	GG 96 × 48
Center for Ocean Land Atmosphere Studies, USA (COLA)	Spectral	R40	Sigma	18	GG 128 × 102
Commonwealth Scientific and Industrial Research Organisation, Australia (CSIRO)	Spectral	R21	Sigma	9	GG 64 × 56
Colorado State University, USA (CSU)	Finite Difference	4 × 5	Modified Sigma	17	LL 72 × 46
Dynamical Extended Range Forecasting at GFDL, USA (DERF)	Spectral	T42	Sigma	18	GG 128 × 64
European Centre for Medium Range Weather Forecasts (ECMWF)	Spectral	T42	Hybrid	19	GG 128 × 64
Goddard Laboratory for Atmospheres, USA (GLA)	Finite Difference	4 × 5	Sigma	17	LL 72 × 46
Goddard Space Flight Center, USA (GSFC)	Finite Difference	4 × 5	Sigma	20	LL 72 × 46
Meteorological Research Institute, Japan (MRI)	Finite Difference	4 × 5	Hybrid	15	LL 72 × 46
Recherche en Prévision Numérique, Canada (RPN)	Spectral	T63	Sigma	23	GG 192 × 96
The UK Universities' Global Atmospheric Modelling Programme, UK (UGAMP)	Spectral	T42	Hybrid	19	GG 128 × 64
United Kingdom Meteorological Office, UK (UKMO)	Finite Difference	2.5 × 3.75	Hybrid	19	LL 96 × 73

Typically, these fields are variances which are filtered to retain synoptic time scales (periods from about two to six days). This technique is not particularly suitable for isolating cyclone behaviour since anticyclones as well as cyclones contribute to the variance. Rogers (1997) gives an example of filtered variance for the winter MSLP field averaged over 1951–1990. If this is compared to one of the standard cyclone event climatologies; e.g. Petterssen (1956), it can be seen that the maxima in the two fields do not agree well. The filtered variance misses the Gulf of Alaska and Mediterranean centres and displaces the Icelandic centre to the west.

Clearly, there is no ideal procedure for identifying cyclones. Even if manual counting were a viable option, it too, is not without difficulties. Typically climatologies are the accumulation of the work of many analysts which can result in a lack of homogeneity in the results. For the present study, it was decided to adopt the simple and economical objective scheme described in Lambert (1988) to produce cyclone event climatologies described previously. Its simplicity leads to the inclusion of spurious events and no attempt is made to exclude them during application of the procedure. It was felt that a scheme which enumerates all true events and includes some spurious events is preferable to a scheme that uses a subjectively determined threshold to give a balance between correctly removing spurious events and erroneously removing real events. Incipient lows, such as those resulting from lee cyclogenesis, are especially at risk of being excluded from the analyses if a threshold is applied.

Despite the simplicity of the scheme described, it was shown in Lambert (1988) that, when applied to observation-based data, it produced a climatology that was quantitatively and qualitatively similar to the standard event climatologies; e.g. Petterssen (1956). In this scheme, the criterion for a cyclone event is the occurrence of a grid point value of MSLP that is lower than each of its four nearest neighbours. For each event, the grid coordinates and the MSLP at the centre grid point are noted. The influences of spurious events can be partially accounted for by noting that they tend to be associated with geographical features making their identification straightforward on geographical displays. In addition, spurious lows tend to be weak so that they will not likely influence statistics on moderate or strong cyclone events.

Using twice-daily polar stereographic MSLP fields, the total number of cyclone events over a 120 day winter period for each model and the observation-based data were computed. Since each grid cell of the polar stereographic grid used is roughly 380 km on a side, the event totals are the number of events per 145 000 km². Following the advice of Hayden (1981), no adjustment of the event totals arising from the changing area of polar stereographic grid squares as a function of latitude is made. For the Northern Hemisphere, the winter period commenced on November 16 resulting in nine winters during the period January 1979 and December 1988 and for the Southern Hemisphere there were ten winter periods beginning on May 17. Since the data for COLA and DERF models were available only once per day, the extracted event totals were doubled.

5 Results

5.1 Climatological winter MSL pressure field

The December-January-February (DJF) MSLP mean for the extratropical Northern Hemisphere was computed for each of the models as well as the average over all the models. It was noted in Lambert and Boer (2001) that the model mean is an important field to consider since it compares very favourably to observations and is often better than any of the individual models. The model mean is displayed in Fig. 1 as a contoured field with the departure from the ECMWF/ERA reanalysis shaded. The model mean is reasonably successful in

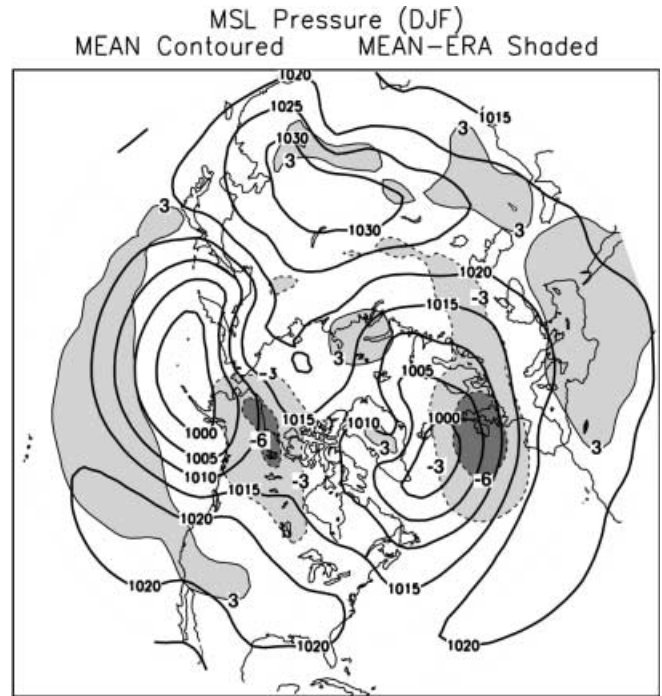


Fig. 1 The simulated Northern Hemisphere mean sea level pressure field averaged over the thirteen AMIP1 models for December–January–February in millibars (contoured) and its departure from the ECMWF/ERA analyses in millibars (*shaded*)

reproducing the MSLP climatology. The semi-permanent features such as the Aleutian Low, the Icelandic Low, and the Siberian High are particularly well simulated. The largest departures of the model mean from the observed field occur over northwestern Canada, off the British Isles, over the Mediterranean, and north of Hawaii. The corresponding results for the Southern Hemisphere winter, June–July–August (JJA), are given in Fig. 2. Again, the model mean is quite successful in simulating the observed climatology. The largest differences occur over the high terrain of Antarctica and are mainly an indication of the different techniques used to extrapolate below ground. Smaller differences occur in the south Pacific Ocean near the coast of Antarctica, the south Indian Ocean near the coast of Antarctica and north of the circumpolar trough near New Zealand and South America suggesting that the intensity of the trough is well simulated but positioned slightly too far north.

The systematic behaviour of the models in simulating the Northern Hemisphere DJF MSLP climatology is given in Fig. 3. The contoured values are the observed (ECMWF/ERA) MSLP. The shaded values give the number of models which exhibit a departure from the observations of a like sign. Positive values indicate that the model simulations are systematically higher than the observations and negative values indicated a negative systematic error. For example, a value of –11 indicates that 11 of the 13 models simulate values of MSLP which are lower than those observed. The strong correspon-

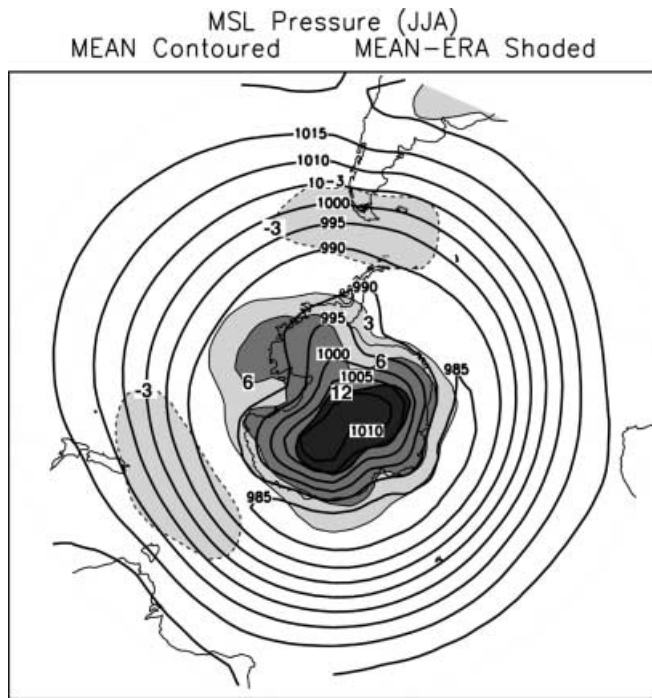


Fig. 2 Same as Fig. 1, except for the Southern Hemisphere for June–July–August

dence between the shadings of Figs. 1 and 3 indicates that the models exhibit a significant similar error in the simulation of the MSLP field.

The corresponding results for the Southern Hemisphere are displayed in Fig. 4. As was the case for the Northern Hemisphere, the models exhibit a noticeable systematic error concentrated in regions where the error in the model mean was also large.

5.2 Cyclone frequencies

The model mean cyclone event climatology was computed by averaging the number of events over all the models. The 120-day Northern Hemisphere winter result is displayed in Fig. 5. The corresponding observed event climatology based on the ECMWF/ERA reanalyses is given in Fig. 6 and that based on the NCEP/NCAR reanalyses in Fig. 7. The figures give the total number of events for the nine winters. During the nine-winter period, 2160 analyses were used to produce the climatologies and dividing the totals by this number gives the fraction of time that a grid point experienced a cyclonic event.

The model mean reproduces the geographical distribution of the observed event climatology rather well. In general, the intensity and position of the Pacific storm track are well simulated. However, the number of simulated events in the vicinity of Japan is lower than observed. The models also fail to weaken the storm track in the Gulf of Alaska allowing too many cyclones to move into northern Canada. The southern edge of the

Consistency of Model Departures From Observations MSLP Pressure (DJF)

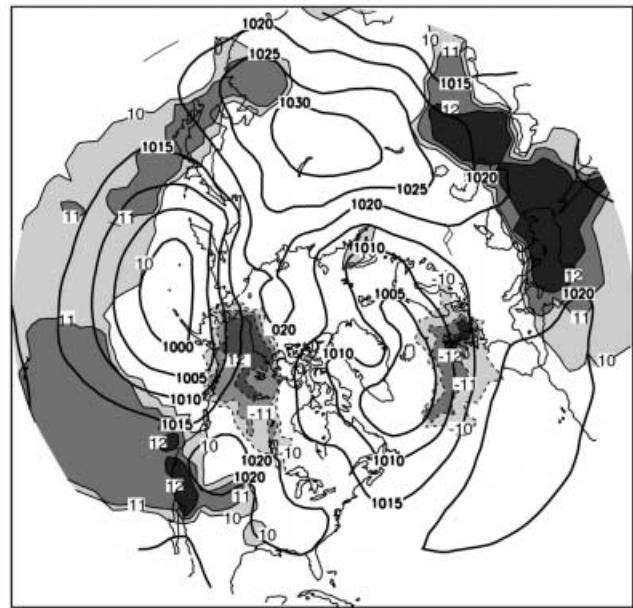


Fig. 3 The shaded values are the number of models exhibiting differences between the model simulation and the observed values of mean sea level pressure for December–January–February of like signs. Positive values give the number of models for which the simulated MSLP is higher than observed and negative values give the number of models which simulate lower values than observed. The contoured values are the ECMWF/ERA analysis of the MSLP field (mb)

mid-ocean portion of the storm track is simulated too far to the north. These two deficiencies are reflected in the model mean MSLP being too low over northwestern Canada and too high north of Hawaii (see Fig. 1).

The main features of the Atlantic storm track are also reasonably well simulated. The model results clearly show the splitting of the track near Greenland and the maxima west of Greenland, near Iceland and north of Scandinavia. It must be kept in mind that there are two sources of spurious events in the Greenland area. The first occurs over the high terrain of Greenland and the second to the west, over Baffin Bay. The maximum over Baffin Bay consists of both real events caused by migratory cyclones moving into the region and spurious events arising from the surface component of the semi-permanent winter upper level cyclone in this area. (The concentration of spurious events in this area is reflected in the noticeable differences between the NCEP and ERA analyses.) Some details of the track are not well simulated. Its position off the coast of the United States is too far to the east and the southern edge of the storm track in the eastern Atlantic is simulated too far south resulting in increased cyclonic activity over the British Isles. This is also consistent with the model mean MSLP being lower than observed in this area.

The models have difficulty in simulating the cyclonic activity in the Mediterranean. The observation-based

Consistency of Model Departures From Observations MSL Pressure (JJA)

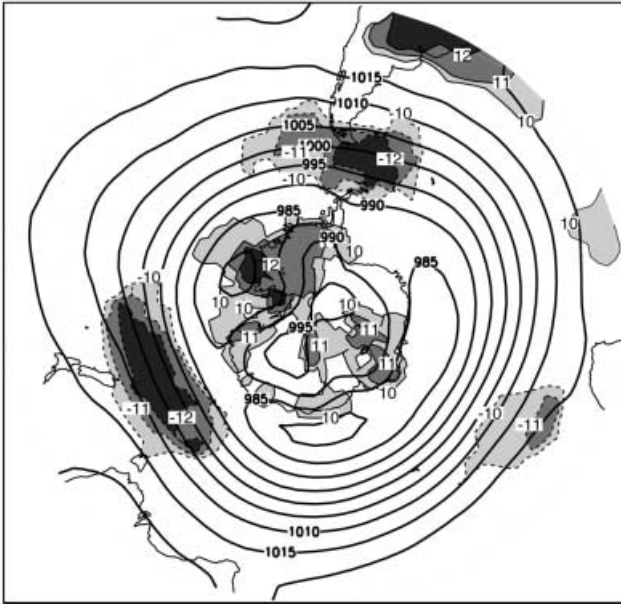


Fig. 4 Same as Fig. 3 except for the Southern Hemisphere for June–July–August

results display a well-defined track with local events occurring nearly five percent of the time. The model mean shows a weak relatively poorly defined track in the Mediterranean. This lack of cyclonic activity is consistent with the higher than observed climatological MSLP in this area as seen in the model mean (Fig. 1). The reduced number of cyclones in the lee of the Alps and in the lee of the Rockies suggest that the models have difficulty in simulating lee cyclogenesis. The increased cyclone activity over large open bodies of water such as the Black Sea, Caspian Sea and the Great Lakes is well simulated.

The fact that excess numbers of cyclones are able to move inland from the Gulf of Alaska and the poor simulation of lee cyclogenesis points to possible difficulties with the topography. If this were the case, then one might expect the high-resolution models to fair better than the low-resolution ones because the former are able to resolve the topography better. This hypothesis was examined and it was found that the behaviour of the models was not resolution dependent or, alternatively, none of the models has sufficient resolution to simulate lee cyclogenesis adequately.

A measure of the individual models' ability to reproduce the observed event climatology can be obtained by computing the spatial correlation coefficient between each model result and that based on the ECMWF/ERA analyses. Figure 8 displays the correlation coefficient over the area from 30° N to the North Pole. The individual model results and the observed result were smoothed using a nine-point filter before the correlations were computed.

Winter Cyclone Events MEAN

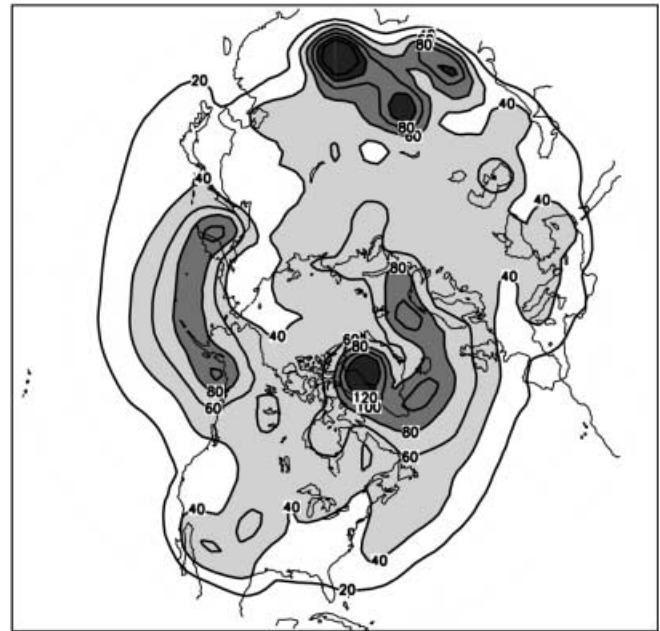


Fig. 5 The number of simulated cyclone events per 145,000 km² accumulated over nine 120 day winter periods for the Northern Hemisphere and averaged over the 13 models

The 90° sector from 30° E to 120° E exhibits many spurious events due to the extrapolation required to compute the MSLP over high terrain. Consequently, this sector is not included in the computation of the correlation. Since few mid-latitude cyclones are observed here, there will be little effect on the results. Greenland is another area of high terrain which has the potential to produce spurious events. Greenland lies astride the Atlantic storm track and is an area of high activity and its high terrain prevents cyclones from penetrating inland. The depiction of the topography by the individual models is resolution dependent which will affect the inland penetration of model cyclones. For these reasons, it is not possible to exclude the spurious events caused by reduction to sea level over Greenland from the computations.

Also included in Fig. 8 are results for the model mean, the NMC operational analyses, and the NCEP/NCAR Reanalyses.

Definitive conclusions should not be drawn from the results of Fig. 8 because of the difficulties in representing a complex field by using a single number. The model mean exhibits a correlation higher than any of the individual models. For the individual models, the ECMWF and the UGAMP (which are related by a common ancestor) exhibit the highest correlations (near 0.9) with the observed climatology and the CSU the lowest (0.63). There is a suggestion that increased resolution improves model simulations of the event climatology even though the two high-resolution models do not exhibit the highest correlations. Also evident is the similarity in the results for the ECMWF and the UGAMP

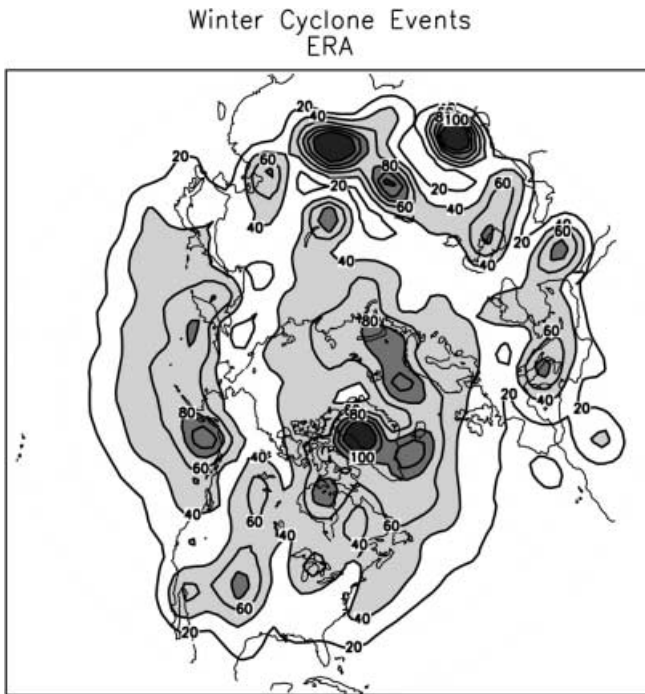


Fig. 6 The number of observed cyclone events per 145,000 km² accumulated over nine 120 day winter periods for the Northern Hemisphere based on the ECMWF/ERA analyses

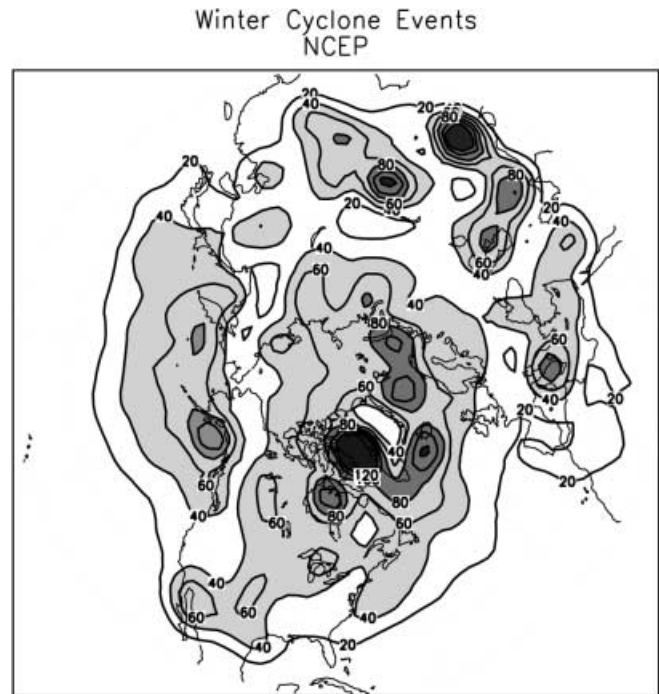


Fig. 7 Same as Fig. 6 except for the NCEP/NCAR analyses

models and to a lesser extent for the GLA and the GSFC models.

If it is assumed that the temporal average of the MSLP field results from contributions from both cyclones and anticyclones, then it is reasonable to assume that the systematic errors in the simulated climatological MSLP field might be accompanied by an excess or deficit of cyclone or anticyclone events or both. In order to examine this, an areal average of the number of cyclone events for each of the models and the ERA analyses was computed by averaging over the grid point values north of 30° N. Using these values, each model's departure from its areal average was computed at each grid point. The resulting departures were used to calculate a mean over all the models. The difference between the model mean departure and the ERA analysis departure for the cyclone events is shown in the left panel of Fig. 9. A corresponding result was obtained for the anticyclone events and this is shown in the right panel of Fig. 9. The anticyclone event departures from the observed departures (right panel) show a band of lower-than-observed events over central Europe and Asia with a band of higher-than-observed events directly to the south. This suggests that the level of anticyclone activity is reasonable but the anticyclone “track” is positioned too far to the south. Another band of lower-than-observed anticyclone events is present over North America. Since this band is not flanked by higher than observed events, it likely results from a failure of the models to simulate the correct level of anticyclonic activity in this region.

The cyclone event departures from observations (left panel) tend to be negatively correlated with the anticyclone event departures. The results also indicate that the models have difficulty in simulating lee cyclogenesis as shown by the paucity of cyclone events to the south of the Alps and to the east of the Rockies. It is also evident that the models fail to simulate the correct level of synoptic activity over much of North America as shown by the low levels of both cyclone and anticyclone events.

The preceding results do point to a relationship between errors in simulating the climatological MSLP field and the error in the number of simulated events. The region near Alaska and northwestern Canada is frequented by lows moving inland from the Gulf of Alaska and Arctic highs which originate over the Beaufort Sea and move southeastwards. Observations indicate that the anticyclonic activity dominates. The simulations on the other hand generally produce the opposite result and this imbalance gives rise to the lower-than-observed MSLP in this area. There is a suggestion from Fig. 9 that the paucity of anticyclone events is more important than the excess of cyclonic ones in this area. This suggests that the physical mechanisms which are responsible for the development of Arctic anticyclones have not been accounted for in the models. The systematic error over and to the west of the British Isles is somewhat different in character. The models simulate the position of the event maximum in the Atlantic storm track correctly but the edge of the track is too far south. This results in the anticyclone events being displaced somewhat to the south. As mentioned previously, the systematic error in the Mediterranean is con-

Fig. 8 The spatial correlation coefficients between the simulated cyclone events and the ECMWF/ERA cyclone events for the 13 models and two analyses for Northern Hemisphere winter

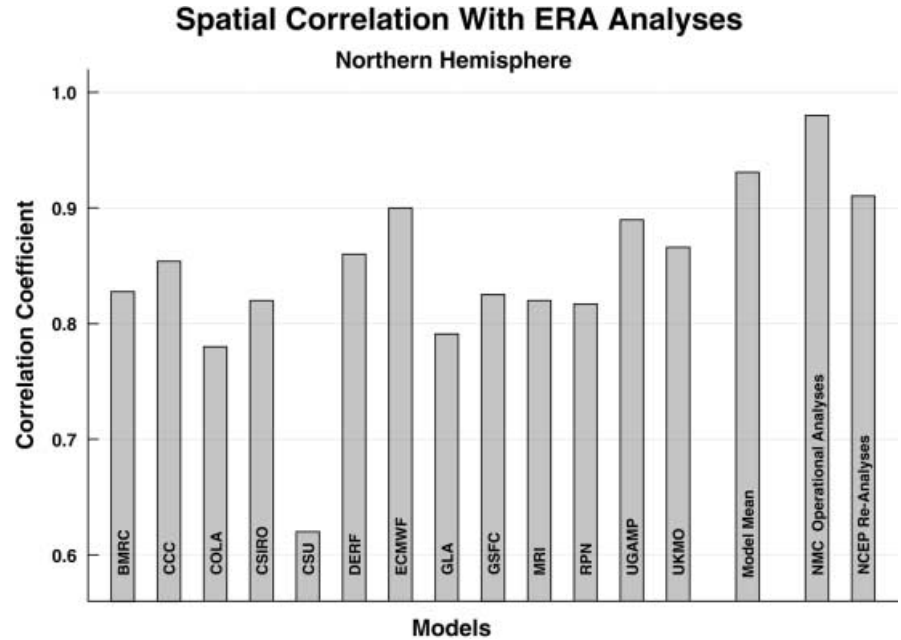
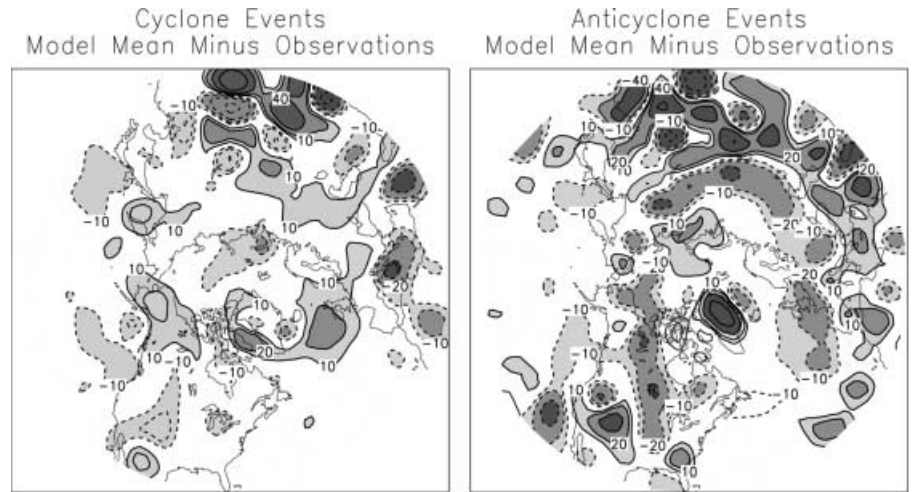


Fig. 9 The difference between the model mean simulated cyclone events and the number of cyclone events from the ECMWF/ERA analyses (*left panel*) and the difference between the model mean simulated anticyclone events and the number of anticyclone events from the ECMWF/ERA analyses



sistent with a deficit of cyclone events resulting from weak lee cyclogenesis.

The number of cyclone events averaged over all the models for the Southern Hemisphere is given in Fig. 10 and the observation-based results of ECMWF/ERA in Fig. 11 accumulated over ten 120 day winters. (No results based on the NCEP/NCAR reanalyses are given because of a processing error in the MSLP field.) During the ten-winter period, 2400 analyses were used to produce the climatology. The fraction of the time that a grid point experiences a cyclone event can be found by dividing the total number of events by 2400.

As Simmonds and Keay (2000) point out, there are no significant mountain barriers in the westerlies and virtually no land-sea temperature contrasts in the Southern Hemisphere which results in a more zonally symmetric event climatology than in the Northern Hemisphere. The observed climatology is characterized

by a circumpolar ring of elevated numbers of events. The only suggestion of a storm track begins in the Tasman Sea and merges with the circumpolar ring. These features are also present in the model mean climatology. However, the simulated circumpolar ring is more intense and slightly farther north than the observed and the simulated Tasman Sea storm track is more diffuse and slightly farther downstream than observed which suggests that the simulated westerlies are too strong. This is consistent with the 200 mb zonal wind comparisons given in Gates et al. (1999).

The spatial correlation coefficients for the individual models are displayed in Fig. 12. The values are computed over all longitudes and from 30° S to the South Pole. The Southern Hemisphere correlations tend to be lower than those of the Northern Hemisphere, even though the former has a simpler spatial structure. The model mean exhibits the highest correlation with

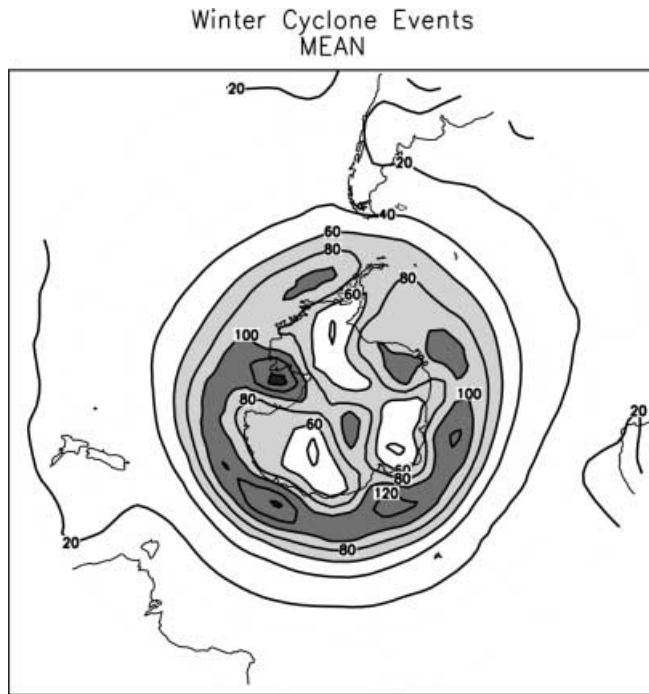


Fig. 10 Same as Fig. 5 except for the Southern Hemisphere

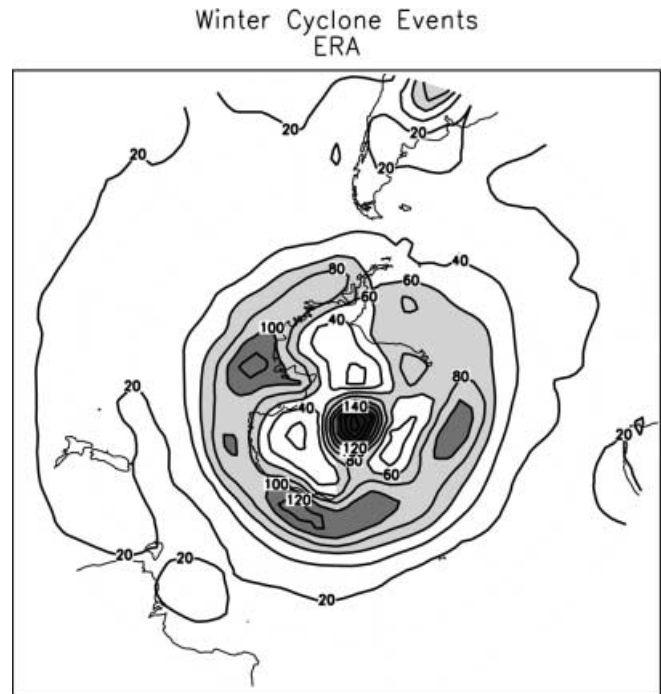


Fig. 11 Same as Fig. 6 except for the Southern Hemisphere

the ECMWF/ERA analyses. The highest correlations for individual models are exhibited by ECMWF and UGAMP and the lowest correlation is exhibited by GSFC. It is also interesting to note the results for the NCEP/NCAR reanalyses and the NMC operational analyses. Both these datasets have known problems as discussed by Trenberth and Olson (1988) and Kistler et al. (2001) with the unfortunate result that these analyses are not able to reproduce the event climatology as well as the ECMWF and UGAMP models can simulate it. There is a noticeable difference in the behaviour of the two dependent pairs, GLA/GSFC and ECMWF/UGAMP. The results for the first pair are quite different and the results for the second pair are quite similar.

5.3 Cyclone intensities

The preceding results have not considered the central pressures of the cyclone events. The events, stratified according to central pressure, give an indication of how well the models are simulating the life cycles of cyclones. Table 2 gives the number of events and the number of events expressed as a percentage of the total number of events in 10 mb intervals from both the ECMWF/ERA reanalyses and the NCEP/NCAR reanalyses accumulated over the nine winters for the Northern Hemisphere and the ten winters for the Southern Hemisphere. This provides an opportunity to intercompare the two datasets for the Northern Hemisphere and to see the effect of the NCEP/NCAR reanalysis difficulties in the Southern Hemisphere. For the Northern Hemisphere, the two

datasets agree remarkably well, except possibly in the weak event categories (those with relatively high central pressures) whose counts include spurious events. In the Southern Hemisphere, the agreement is poor with the lack of agreement being greatest in the strong event categories. This is consistent with the synthetic PAOBS data being incorrectly assimilated in the NCEP/NCAR reanalyses. Much of the PAOBS data would have been used to refine the analysis of deep low pressure systems. Since these data were assimilated in the wrong geographical positions, they tended to be rejected by the quality control procedure, resulting in less well-defined deep cyclones.

The event totals for the individual models were also computed. These totals were then normalized by the number of events computed from the ECMWF/ERA reanalysis dataset and the results for each model are expressed as a fraction of the observed events. Figure 13 gives the results for the Northern Hemisphere. In order to reduce results affected by spurious counts, only events with central pressures of 1000 mb or less are considered. The models exhibit a wide range of behaviour. The most striking results are for GLA and GSFC which produce an ever increasing excess number of events with decreasing central pressure which suggests that dissipation is too weak. As mentioned previously, these two evolved from the same model and many of their features are similar. Neither model employs gravity wave drag nor horizontal diffusion. As mentioned previously, the formulation of the ECMWF/UGAMP pair is even more similar than that of the GLA/GSFC pair. In spite of this, the ECMWF and the UGAMP models behave differently. The ECMWF model simulates more cyclone

Fig. 12 Same as Fig. 8 except for the Southern Hemisphere

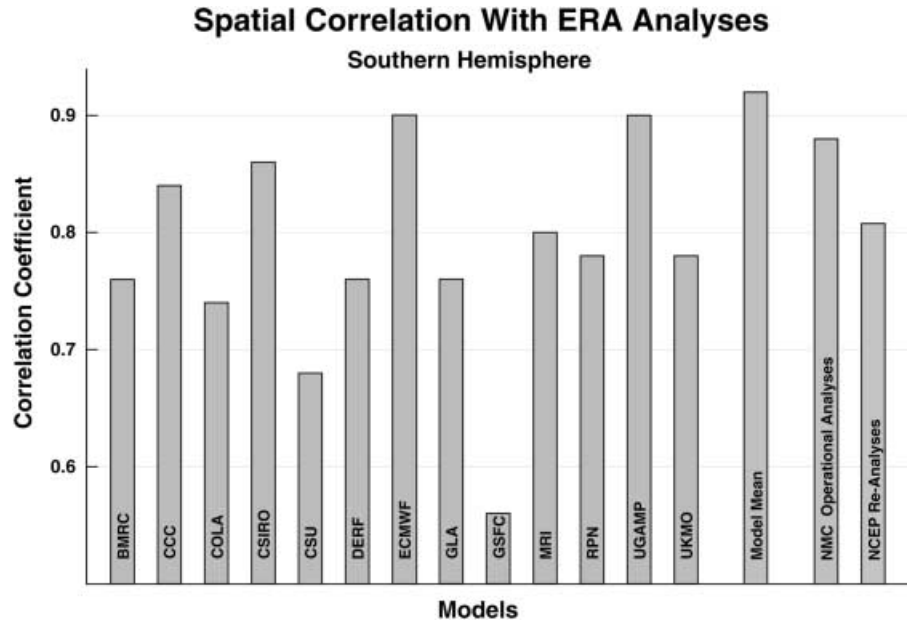


Table 2 A comparison of the observed cyclone events as a function of central pressure from two reanalysis datasets

OBS	Central pressure (mb)									
	> 1020	1020 1010	1010 1000	1000 990	990 980	980 970	970 960	960 950	< 950	
Northern Hemisphere (nine-winter totals)										
ERA	Number	4085	10892	10807	7627	5217	2850	1066	235	48
	Percent	9.5	25.4	25.2	17.8	12.2	6.7	2.5	0.5	0.1
NCEP	Number	4180	10562	11598	7990	5220	2853	1062	229	43
	Percent	10.2	25.7	28.3	19.5	12.7	7.0	2.6	0.6	0.1
Southern Hemisphere (ten-winter totals)										
ERA	Number	370	2830	4444	4851	6293	7461	5656	2634	820
	Percent	1.0	8.0	12.6	13.7	17.8	21.0	16.0	7.4	2.3
NCEP	Number	582	3218	4922	6231	8106	8465	5155	1586	247
	Percent	1.5	8.4	12.8	16.2	21.0	22.0	13.4	4.1	0.6

events than observed and the UGAMP model too few. According to the description given in Phillips (1994), the two models differ in their convective parametrizations and their horizontal diffusion with UGAMP being the more diffusive model. However, without further analysis it is too speculative to attribute differences in model behaviour to differences in model formulation. Except for very deep cyclones, the ratio of simulated to observed events in each bin is relatively constant for BMRC, CCC, CSU, ECMWF, MRI, UGAMP, and UKMO giving a “flat” spectrum. In general, the remaining models (COLA, CSIRO, DERF, and RPN), simulate too few cyclone events with the deficit becoming increasingly larger with decreasing surface pressure. There is no obvious relationship between number of events simulated by a model and its resolution. In fact, it is interesting to note that the behaviour of the model with the highest resolution (RPN) is very similar to that of the model with the lowest resolution (CSIRO).

The corresponding Southern Hemisphere results are given in Fig. 14. Only one model, ECMWF, exhibits a reasonably flat spectrum. As mentioned previously, this likely does not result from the use of the ECMWF/ERA analyses for verification. Three of the models, GLA, UGAMP, and UKMO, simulate an increasing excess of cyclone events with decreasing central pressure. The remaining models, BMRC, CCC, COLA, CSIRO, CSU, DERF, GSFC, MRI, and RPN, tend to simulate too many weak events and insufficient numbers of strong events yielding spectra that have a considerably steeper negative slope than the corresponding spectra for the Northern Hemisphere. It is interesting to note the difference in behaviour of the GLA and GSFC models. In the Southern Hemisphere, these models behave very differently. GLA simulates too many strong events while GSFC simulate too few. As was the case for the Northern Hemisphere, resolution does not appear to influence the distribution of events as a function of central pressure.

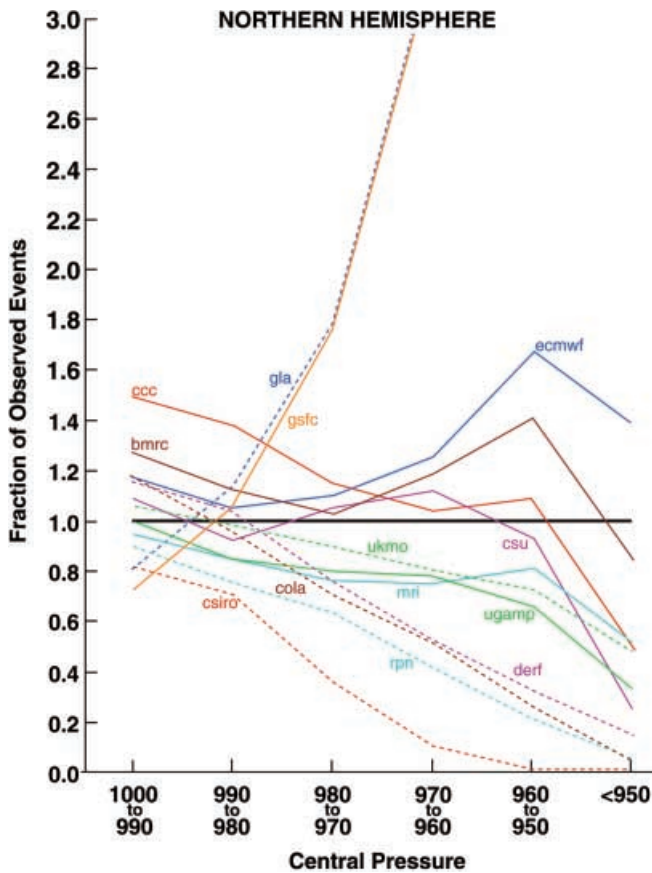


Fig. 13 The number of Northern Hemisphere winter cyclone events as a function of central pressure. The values are normalized by the ECMWF/ERA values

We have presented measures of the ability of the AMIP1 models to reproduce the observed geographical distribution of the cyclone event climatology and the distribution of cyclone events as a function of central pressure. It is not clear how these two measures could be combined to rank the success of the model simulations or indeed if it is appropriate to do so. A subjective assessment of the Northern Hemisphere results, based on the measures mentioned, suggests that the best performing models are UKMO, UGAMP, ECMWF, and BMRC and for the Southern Hemisphere are UGAMP, ECMWF, CSIRO, and CCC.

5.4 Interannual variability

A few studies have examined the interannual variability in the simulations of particular models forced by observed boundary conditions; e.g. Straus and Shukla (1997) and May and Bengtsson (1998). The AMIP1 exercise provides an opportunity to examine the interannual variability in a wide range of models forced with the same observed boundary conditions.

The interannual variability in the number of cyclone events is expressed as anomalies computed as a

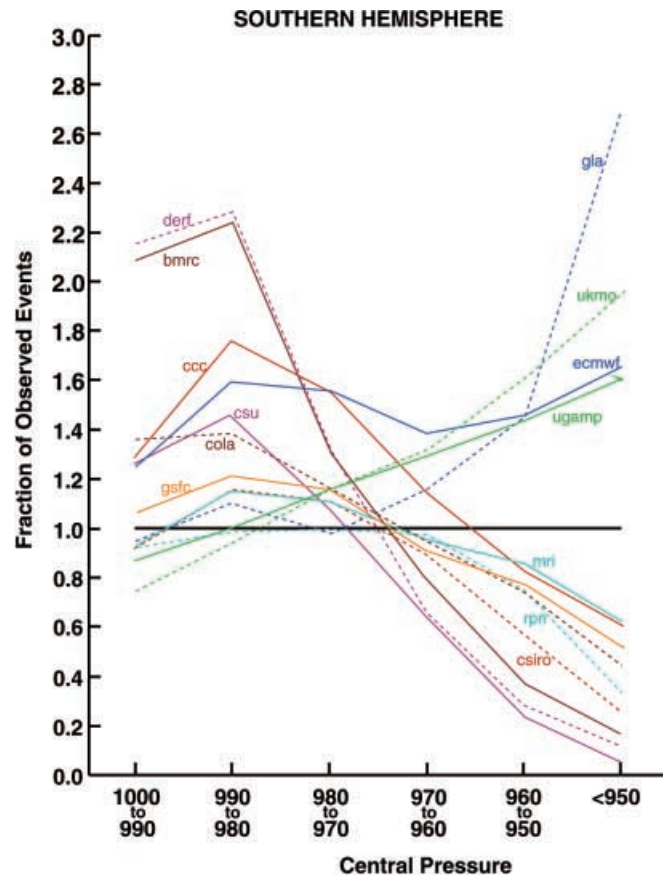


Fig. 14 Same as Fig. 13 except for the Southern Hemisphere

percentage departure from the nine-winter mean. The observed Northern Hemisphere anomalies for the number of cyclone events in 10 mb bins for each winter season is given in Fig. 15. The interannual variability is relatively low for events with central pressures greater than 980 mb. For events with lower central pressures, the interannual variability becomes much larger. This suggests that although the number of moderate cyclones is relatively constant each year, there is a large interannual variability in the number of moderate cyclones which deepen to become intense cyclones. As was mentioned previously, there is an ENSO signal in the number of intense Northern Hemisphere winter cyclone events (Lambert 1996). It could be speculated that the increase in temperature in the tropics increases the pole to equator temperature gradient and consequently increasing the baroclinicity of the atmosphere favouring increased cyclonic activity. In addition, the increase of temperature in the tropics increases the evaporation providing a greater supply of water vapour for transport into the mid-latitudes resulting in increased latent heat release and contributing to the deepening of cyclones. The ENSO signal is evident from Fig. 15 which shows an increase in intense cyclone events during the winters of 1982/1983 and 1986–1987 both of which were El Niño years and a decrease in 1980/1981 and 1984/1985 which were La Niña years. Since the models have been forced

Observed Cyclone Event Anomalies

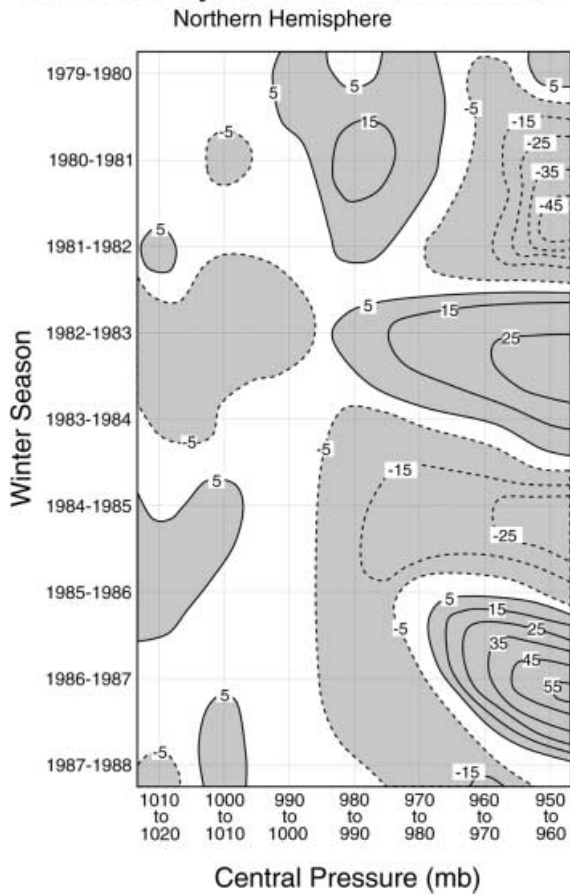


Fig. 15 The observed individual winter cyclone event anomalies for the Northern Hemisphere north of 30°N expressed as a percentage of the nine-year winter mean

with the observed SSTs, this signal provides an opportunity to determine if the models are responding correctly to the interannual variability in the forcing. We assess the models' performance by computing the temporal correlation between the simulated and observed number of cyclone events with central pressures less than 960 mb for: (a) the Northern Hemisphere north of 30° N, (b) the Pacific sector (110° E–120° W) and (c) the Atlantic sector (80° W–50° E). The hemispheric results are displayed in Fig. 16 as wide heavily shaded bars. As a result of the paucity of intense cyclones simulated by the CSIRO model, statistics for this model may well suffer from sampling problems. The results for the model mean (not shown) exhibit a very weak correlation with the observations indicating that, as a group, the performance of the models is rather disappointing. Most exhibit weak or negative correlations with the observations. Only the ECMWF model and possibly the MRI model display reasonable positive correlations. The large number of negative correlations suggests that many of the models respond to the imposed SSTs and sea-ice extent but the response is opposite to that of the real atmosphere. Studies indicate that the Aleutian Low and the Icelandic Low respond differently to ENSO. Bengtsson et al. (1996) describe a multi-year simulation made with imposed SSTs. They noted a strengthening of the Aleutian Low but a weakening of the Icelandic low during the positive phase of ENSO. This out-of-phase response raises the possibility that negative hemispheric correlations exhibited by the models may result from an incorrect response in only one sector. The Pacific and the Atlantic correlations are shown as lightly shaded bars flanking the hemispheric results. The Atlantic results are labelled with an "A" at the tip of the bars and the Pacific

Fig. 16 Temporal correlation coefficient between the model time series of intense (central pressures below 960 mb) cyclone event anomalies and the time series of observed intense cyclone event anomalies for the Northern Hemisphere north of 30°N

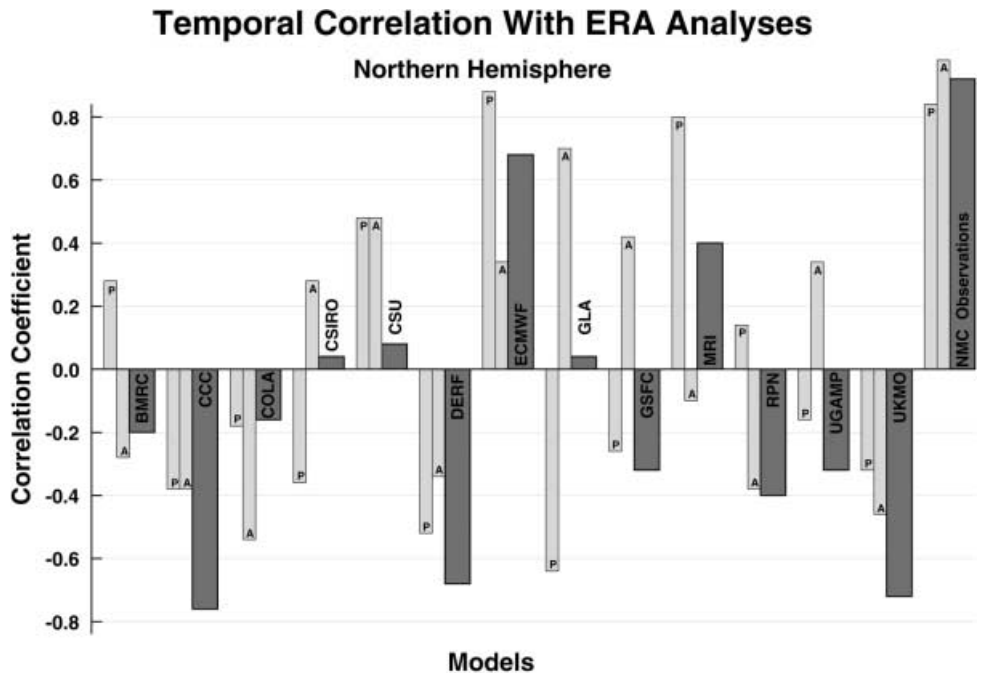




Fig. 17 Same as Fig. 15 except for the Southern Hemisphere south of 30°S

results with a “P”. Those models which exhibit the largest negative hemispheric correlations, (CCC, DERF, UKMO) respond in the same sense in each of the individual sectors.

The corresponding observed anomalies for the Southern Hemisphere are given in Fig. 17. In the Southern Hemisphere, the interannual variability is more uniformly distributed with central pressure than in the Northern Hemisphere. There is no obvious ENSO signal in these results and it is possible that the interannual variability in the SST field does not bring about large changes in the number of cyclone events in the Southern Hemisphere. If this is the case, then the observed interannual variance in the number of events is more chaotic in nature and one should not expect the models to reproduce this variability well. Figure 18 gives the correlation between the model simulations and the observations. In general, the correlations are weaker than in the Northern Hemisphere which also suggests that the models, like the atmosphere, do not exhibit a noticeable response to the SSTs and sea-ice extent. It is interesting to note that the ECMWF model is negatively correlated with the ERA analyses which is further evidence that the ECMWF model does not benefit from the use of the ERA analyses for verification.

In general, only one AMIP1 realization was available for each model and it is not possible, in general, to assess how robust the results would be for a series of simulations. However, for the CCC model, multiple realizations were available presenting an opportunity to examine the consistency of the results obtained from different realizations. For each of six simulations, slightly different initial conditions were used with the same SSTs and sea-ice extent. Intense event anomalies for each Northern Hemisphere winter season were

Fig. 18 Same as Fig. 15 except for the Southern Hemisphere south of 30°S

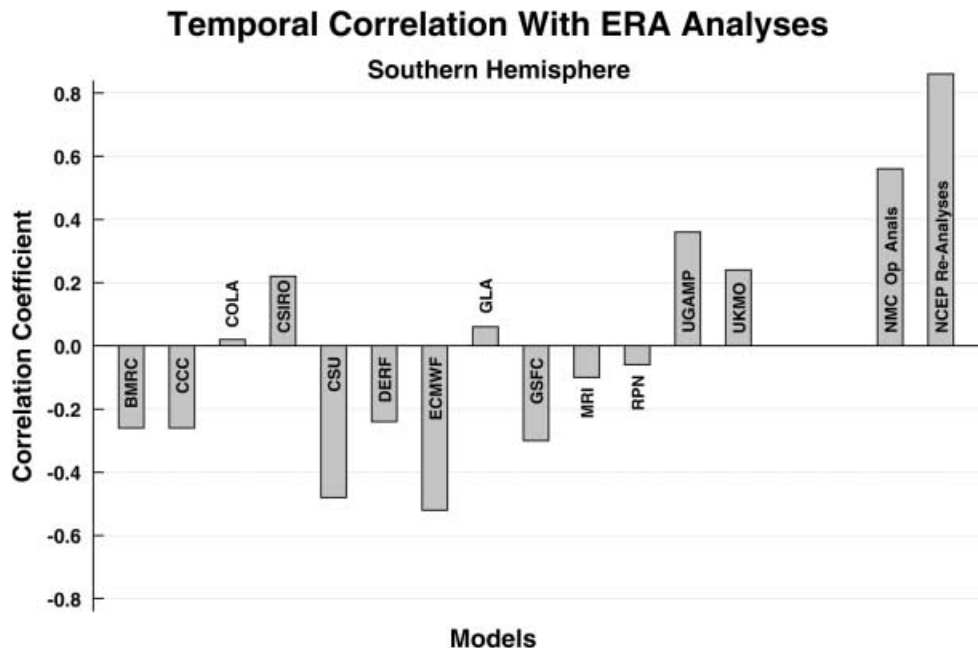
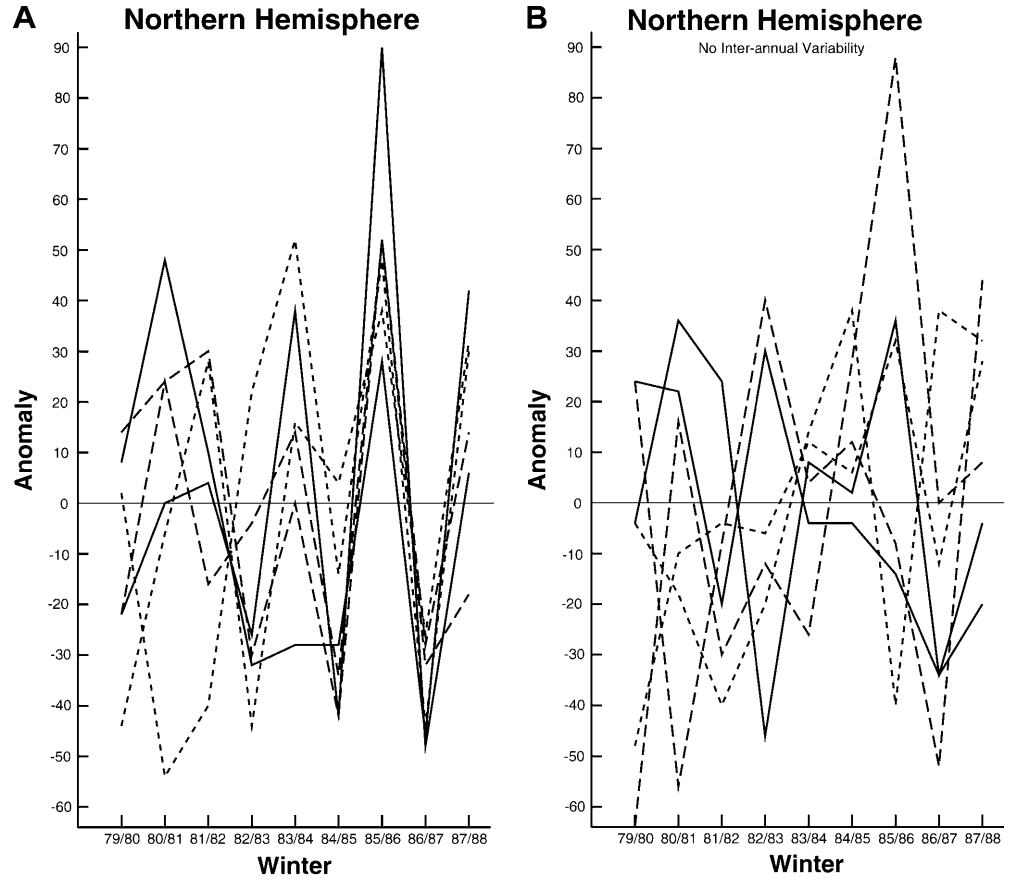


Fig. 19 **A** The anomalies for cyclone events with central pressures below 960 mb for six realizations using the CCC model. **B** The anomalies for cyclone events with central pressure less than 960 mb for six realizations which have no interannual variability in the SST and sea-ice forcing



computed for each of the six experiments. The anomalies were computed as a departure of the number of intense cyclone events in each winter from the nine-winter mean. The results are displayed in Fig. 19a. During the last six winters, at least five of the six experiments agree on the sign of the anomalies. For the CCC model six additional AMIP-like experiments were carried out with no interannual variability in the SSTs and the sea-ice extent. The six experiments were done using slightly different initial conditions and forced by the mean of the SSTs and sea-ice extent. These results are given in Fig. 19b. As would be expected the results are more random. In no winter do all six simulations produce the same anomaly. Taken together, the two sets of results suggest that the CCC model does respond consistently to the imposed SSTs. However, as was seen previously, the model response and the observed atmospheric response to the SSTs and sea-ice extent are strongly negatively correlated.

6 Summary

Various aspects of the simulated behaviour of cyclones in thirteen models participating in the AMIP1 exercise are presented. In the simulation of the winter climatological MSLP field for the Northern Hemisphere, the models produce reasonable simulations of the “semi-permanent” features of the climatology. The greatest

departures from the observed climatology occur over northwestern North America, over and to the west of the British Isles and in the Mediterranean. The departures in the three geographical areas are very systematic in that at least eleven of the models exhibit similar departures from observations. A similar situation was seen in the Southern Hemisphere where, on average, the circumpolar trough was well simulated, albeit somewhat too far north, with systematic errors near Africa, New Zealand, and South America.

The simulations of the cyclone events showed that the models are reasonably successful in reproducing the large-scale geographic aspects of the observed cyclone events but deficiencies in the details of the simulations are apparent. The paucity of simulated events to the south of the Alps and to the east of the Rockies suggests that the models have difficulty simulating lee cyclogenesis. Over much of North America, the models have difficulty simulating the correct level of synoptic activity as demonstrated by the low numbers of both cyclone events and anticyclone events.

The models have difficulty simulating the distribution of cyclone events as a function of central pressure. The most common problem is that the models exhibit an ever increasing deficit of events with decreasing central pressure. This defect is larger in the Southern Hemisphere than the Northern Hemisphere and does not appear to be resolution dependent since the behaviour of

the highest resolution model and the lowest are very similar.

There is an apparent ENSO signal in the observed Northern Hemisphere interannual variability of intense cyclone events. With the exception of ECMWF, the models failed to reproduce this phenomenon. There is some evidence that the models do indeed respond to the interannual variability in the SSTs, but the response is out of phase with that of the atmosphere. In the Southern Hemisphere, there does not appear to be ENSO-induced interannual variability in the observed numbers of cyclone events. It could be argued that the models have been reasonably successful in the Southern Hemisphere since they too do not exhibit any ENSO-induced interannual variability.

There were six AMIP experiments with the CCC model. The response, as measured by anomalies of intense Northern Hemisphere winter cyclone events, was remarkably consistent for the six cases. Six additional realizations used the CCC model in which there was no interannual variation in the SSTs and sea-ice extent. In this set of experiments, the response was much more random. This set of simulations indicates that the CCC model does indeed respond to the imposed SSTs and sea-ice extent. Since multiple realizations for other models were not available, one cannot say if the response seen in the CCC model would be exhibited by others. It would also be interesting to determine how sensitive the response is to model formulation. For example, if minor changes were made to the CCC model and a series of AMIP simulations were made, would the model still respond in a consistent way and how different would the response be compared to that of the unchanged model? If we assume, as a result of their similarity, that the GSFC model is a modified GLA model and the UGAMP model is a modified ECMWF model, then there is a suggestion that the model response is sensitive to formulation.

The results of this study support the need for multiple realizations of AMIP simulations in order to verify the robustness of model responses. The model intercomparison process would benefit from a stronger interaction between the diagnostic groups and the modelling groups and perhaps a willingness of the modelling groups to perform experiments to attempt to answer attribution questions. The AMIP2 exercise which is currently underway has begun to address such extensions to the AMIP experimental design.

Acknowledgements The authors appreciate the substantial efforts of the two referees whose comments greatly improved the manuscript.

References

- Bengtsson L, Arpe K, Roeckner E, Schulzweida U (1996) Climate predictability experiments with a general circulation model. *Clim Dyn* 12: 261–278
- Betts AK, Miller MJ (1994) The Betts-Miller Scheme. In: Emanuel KA, Raymond DJ (eds) *The representation of cumulus convection in numerical models of the atmosphere*. American Meteorological Society, Boston, MA, USA
- Blackmon ML (1976) A climatological spectral study of the 500 mb height of the Northern Hemisphere. *J Atmos Sci* 33: 1607–1623
- Gates WL (1992) AMIP: The atmospheric model intercomparison project. *Bull Am Meteorol Soc* 73: 1962–1970
- Gates WL, Boyle JS, Covey C, Dease CG, Doutriaux CM, Drach RS, Fiorino M, Gleckler PJ, Hnilo JJ, Marlais SM, Phillips TJ, Potter GL, Santer BD, Sperber KR, Taylor KE, Williams DN (1999) An overview of the results of the Atmospheric Model Intercomparison Project (AMIP 1). *Bull Am Meteorol Soc* 80: 29–56
- Gibson JK, Kallberg P, Uppala S, Hernandez A, Nomura A, Serrano E (1997) ECMWF Re-Analysis Project Report 1. ERA Description. ECMWF, Shinfield Park, Reading, UK
- Hayden BP (1981) Cyclone occurrence mapping: equal area or raw frequencies? *Mon Weather Rev* 109: 168–172
- Kalnay E, Kanamitsu M, Kistler R, Collins W, Deaven D, Gandin L, Iredell M, Saha S, White G, Woollen J, Zhu Y, Chelliah M, Ebisuzaki W, Higgins W, Janowiak J, Mo KC, Ropelewski C, Wang J, Leetmaa A, Reynolds R, Jenne R, Joseph D (1996) The NCEP/NCAR 40-year reanalysis project. *Bull Am Meteorol Soc* 77: 437–471
- König W, Sausen R, Sielmann F (1993) Objective identification of cyclones in GCM simulations. *J Clim* 6: 2217–2231
- Kistler R, Kalnay E, Collins W, Saha S, White G, Woollen J, Chelliah M, Ebisuzaki W, Kanamitsu M, Kousky V, van den Dool H, Jenne R, Fiorino M (2001) The NCEP-NCAR 50-year reanalysis; monthly means CD-ROM and documentation. *Bull Am Meteorol Soc* 82: 247–267
- Lambert SJ (1988) A cyclone climatology of the Canadian Climate Centre General Circulation Model. *J Clim* 1: 109–115
- Lambert SJ (1996) Intense extratropical Northern Hemisphere winter cyclone events: 1899–1991. *J Geophys Res* 101: 21,319–21,325
- Lambert SJ, Boer GB (2001) CMIP1 evaluation and intercomparison of coupled climate models. *Clim Dyn* 17: 83–106
- Lau N-G (1988) Variability of the observed midlatitude storm tracks in relation to low-frequency changes in the circulation pattern. *J Atmos Sci* 45: 2,718–2,743
- May W, Bengtsson L (1998) The signature of ENSO in the Northern Hemisphere midlatitude seasonal mean flow and high-frequency intraseasonal variability. *Meteorol Atmos Phys* 68: 81–100
- Petterssen S (1956) *Weather analysis and forecasting*, vol 1. McGraw-Hill, pp 422
- Phillips TJ (1994) A summary documentation of the AMIP models. Report No. 18, PCMDI, PCMDI, Lawrence Livermore National Laboratory, Livermore, USA, UCRL-ID-116384, 343 pp. (Available online at <http://www-pcmdi.llnl.gov/pcmdi/pubs/>)
- Rogers JC (1997) North Atlantic storm track variability and its association to the North Atlantic Oscillation and climate variability of northern Europe. *J Clim* 10: 1635–1647
- Simmonds I, Keay K (2000) Mean Southern Hemisphere extratropical cyclone behavior in the 40-year NCEP-NCAR reanalysis. *J Clim* 13: 873–885
- Sinclair MR, Watterson IG (1999) Objective assessment of extratropical weather systems in simulated climates. *J Clim* 12: 3467–3485
- Straus DM, Shukla J (1997) Variations of midlatitude transient dynamics associated with ENSO. *J Atmos Sci* 54: 777–790
- Taylor KE (1986) An analysis of the biases in traditional cyclone frequency maps. *Mon Weather Rev* 114: 1481–1490
- Tiedtke M (1989) A comprehensive mass flux scheme for cumulus parametrization in large-scale models. *Mon Weather Rev* 117: 1779–1800
- Trenberth KE, Olson JG (1988) Evaluation of NMC global analyses: 1979–1987. NCAR Technical Note, NCAR/TN-299 + STR

- Trigo IF, Davies TD, Bigg GR (1999) Objective climatology of cyclones in the Mediterranean region. *J Clim* 12: 1685–1696
- Wallace JM, Lim G-H, Blackmon ML (1988) Relationship between cyclone tracks, anticyclone tracks, and baroclinic waveguides. *J Atmos Sci* 45: 439–462
- Whittaker LM, Horn LH (1984) Northern Hemisphere extratropical cyclone activity for four midseason months. *J Climatol* 4: 297–310